IOP PUBLISHING PLASMA PHYSICS AND CONTROLLED FUSION

Plasma Phys. Control. Fusion **53** (2011) 045004 (10pp) doi:10.1088/0741-3335/53/4/045004

Low-frequency Alfvén gap modes in rotating tokamak plasmas

J W Haverkort[1,2], **H J de Blank**[1] **and B Koren**[2,3]

[1] FOM Institute for Plasma Physics Rijnhuizen, Association EURATOM-FOM, Trilateral Euregio Cluster, PO Box 1207, Nieuwegein, The Netherlands
[2] Centrum Wiskunde & Informatica (CWI), PO Box 94079, Amsterdam, The Netherlands
[3] Mathematical Institute, Leiden University, PO Box 9512, 2300 RA Leiden, The Netherlands

E-mail: J.W.Haverkort@cwi.nl

Received 9 July 2010, in final form 4 January 2011
Published 24 February 2011
Online at stacks.iop.org/PPCF/53/045004

Abstract

As a result of toroidal rotation, sequences of new global modes are predicted to arise in magnetically confined plasmas. The frequencies of these Alfvén modes lie inside gaps of the continuous magnetohydrodynamic (MHD) spectrum that are created or enlarged by toroidal flow. The numerically obtained results are compared with an analytical investigation, yielding a useful criterion for mode existence. Because of their low frequencies, these modes may be easily destabilized by energetic particles. Because of their sensitivity to the Mach number however, these modes can provide a valuable extension to MHD spectroscopy by giving information on the rotational velocity.

1. Introduction.

In magnetically confined toroidal plasmas, such as tokamak plasmas for fusion energy research, high toroidal flow speeds can arise through neutral beam injection or intrinsic mechanisms. Such flow causes fundamental changes in the magnetohydrodynamic (MHD) stability and wave spectrum of the plasma. Centrifugal forces e.g. can stabilize various otherwise unstable modes [1, 2]. Toroidal rotation most significantly influences the low-frequency part of the spectrum, where at the same time MHD-stable waves are prone to destabilization by fast ions. Understanding the complete MHD spectrum of modes excited by fast ions [3] or antennas [4] is important for diagnostic purposes. Modes that are sensitive to rotation are of particular interest.

Here we present a new class of low-frequency MHD modes that exhibit such sensitivity to toroidal plasma rotation. The modes were found numerically and investigated analytically. Toroidal rotation, plasma compressibility and coupling between Alfvén waves and slow magnetosonic waves are taken into account.

A pronounced consequence of plasma rotation is the appearance of a toroidal flow-induced (TFI) gap in the continuous MHD spectrum [5, 6]. In a toroidal plasma, coupling of Alfvén waves to sound waves gives rise to a second spectral gap [7–9]. This pressure or β-induced Alfvén gap extends to the higher frequency of the geodesic acoustic mode (GAM) [10, 11]. Contrary to singular continuum modes, radially extended 'global' modes may exist within these gaps, with discrete frequencies near an extremum in the continuous spectrum. The radial group velocity of these standing waves vanishes because of interference with either a counter-propagating wave or with its own reflection off some 'potential well' in the plasma [12]. An experimentally well-established example of the first type is the toroidal Alfvén eigenmode (TAE) [13] while the latter category includes the global Alfvén eigenmode [14] and the reversed-shear Alfvén eigenmode (RSAE) [15–17]. Global modes called beta-induced Alfvén eigenmodes (BAEs) [8, 18] can exist near the GAM frequency. Recently, β-induced Alfvén acoustic eigenmodes were found both numerically and experimentally [19]. These modes also occur within the BAE/GAM gap, but at lower frequencies associated with extrema due to slow-Alfvén coupling. Toroidal rotation widens the BAE/GAM gap and a single global toroidal flow-induced Alfvén eigenmode (TFAE) can appear [5, 6].

We show that toroidal rotation can cause the formation of a new class of global Alfvén modes below the BAE/GAM gap, which are distinctly different from both the BAE and the TFAE. Similarly, modes are shown to arise within the TFI gap for sufficient rotation. Observation of such modes that are sensitive to rotation can give detailed information on the rotation velocity, providing a valuable extension to MHD spectroscopy [4, 16, 17]. Using a simplified mode equation, a total of four types of Alfvén modes occurring above and below the TFI and BAE/GAM gap are analysed in a unified way. The analysis is therefore also relevant for the description of RSAEs in rotating plasmas. Simple criteria for mode existence are derived that agree with computations.

2. Preliminaries

We consider an axisymmetric tokamak plasma with major radius R_0, minor radius a and a constant temperature $T \equiv p/\rho$, with p and ρ the plasma pressure and density, respectively. The plasma is assumed to rotate rigidly with a velocity $\boldsymbol{V} = R\Omega\hat{\boldsymbol{e}}_\phi$ at an angular frequency Ω in the toroidal $\hat{\boldsymbol{e}}_\phi$-direction. The geometry of the magnetic field $\boldsymbol{B}$ can be specified in cylindrical coordinates (R, Z, ϕ) in terms of the poloidal magnetic flux function $\psi(R, Z)$, which runs from ψ_m on the magnetic axis to ψ_e at the plasma edge. The pressure $p(\psi, R) = p_0(\psi)\exp(\gamma M(R)^2/2)$, where $M(R) = R\Omega/\sqrt{\gamma T}$ is the Mach number and γ the ratio of specific heats. For constant $P \equiv \mathrm{d}p_0/\mathrm{d}\psi$ and $J \equiv \frac{1}{2}\mathrm{d}(RB_\phi)^2/\mathrm{d}\psi$, the axisymmetric ideal MHD equations can be solved analytically, leading to [20]

$$\psi = c_1 R^2 + c_2 R^2\left(Z^2 - \frac{R^2}{4}\right) - \frac{JZ^2}{2} - \frac{PR_0^4}{\gamma^2 M_0^4}\mathrm{e}^{\gamma M(R)^2/2}, \tag{1}$$

where $M_0 \equiv M(R_0)$. The coefficients c_1 and c_2 depend on the external magnetic field and can be adjusted to yield nested magnetic surfaces ψ.

Next, we perturb this equilibrium with a displacement $\boldsymbol{\xi}(\boldsymbol{r}, t)$ of the rotating plasma. Because of axisymmetry, we can investigate a single toroidal harmonic:

$$\boldsymbol{\xi}(\psi, \vartheta, \phi, t) = \sum_m \boldsymbol{\xi}_m(\psi)\mathrm{e}^{\mathrm{i}(m\vartheta - n\phi - \omega t)}. \tag{2}$$

The angle ϑ is such that in the (ϑ, ϕ)-plane the magnetic field lines are straight. Inserting these perturbations into the linearized ideal MHD equations, a generalized eigenvalue problem can

be obtained for the eigenvalues ω [21] that is solved numerically. The numerical code actually uses an Eulerian velocity perturbation $\boldsymbol{v}$ which, for rigid toroidal equilibrium rotation, is related to $\boldsymbol{\xi}(\boldsymbol{r}, t)$ by $\boldsymbol{v} = -\mathrm{i}(\omega + n\Omega)\boldsymbol{\xi}$.

The problem can be substantially simplified for a tokamak plasma with a circular cross-section and inverse aspect ratio $\epsilon \equiv a/R_0 \ll 1$, when investigating low frequencies $\omega \sim \Omega$ and assuming the ordering $M_0 \sim 1$, $m/q - n \sim \epsilon$, and $\beta \sim \epsilon^2$. Here the plasma beta $\beta = 2p_0 \exp(\gamma M_0^2/2)/B^2$ and the safety factor $q(r) = B^\phi/B^\vartheta$, with r a radial flux coordinate. For non-zero m and n, a mode equation for the radial component of the main harmonic $\xi \equiv \xi^r_{\mathrm{m}}(r)$ can be derived [22] from the Frieman–Rotenberg formalism [23]:

$$\left(r^3 A_1 \xi'\right)' + \left[r^2 A_2' - r(m^2 - 1)A_1\right]\xi = g. \tag{3}$$

Here a prime denotes $\mathrm{d}/\mathrm{d}r$ and at resonance $q = m/n$:

$$A_1 = \frac{1}{2}\gamma\beta q^2 \frac{(\bar\omega^2 - \bar\omega_-^2)(\bar\omega^2 - \bar\omega_+^2)}{1 - \bar\omega^2/\bar\omega_0^2},$$

$$A_2 = A_1 + \beta\left[m^2\left(1 - \frac{\gamma}{2}M_0^2 - \frac{\gamma^2}{4}M_0^4\right) - n^2 + 2\gamma m \frac{\bar\omega/\bar\omega_0}{1 - \bar\omega^2/\bar\omega_0^2} M_0\left(1 + \frac{1}{2}M_0^2\right)\right]. \tag{4}$$

Here $\bar\omega \equiv (\omega + n\Omega)/\omega_{\mathrm{s}}$ denotes the Doppler shifted frequency normalized by $\omega_{\mathrm{s}} \equiv \sqrt{\gamma T}/R_0$ and

$$\bar\omega_\pm^2 = a_1 \pm \sqrt{a_1^2 - a_2} \qquad \text{and} \qquad \bar\omega_0 = 1/q, \tag{5}$$

where

$$a_1 = 1 + \frac{1}{2q^2} + 2M_0^2 + \frac{\gamma}{4}M_0^4 \qquad \text{and} \qquad a_2 = \frac{\gamma - 1}{2q^2}M_0^4. \tag{6}$$

The Mercier term of [22] is here absorbed in A_2. Away from resonance, magnetic shear is taken into account by replacing A_1 with $A_1 + (m/q - n)^2$ in (3). The inhomogeneous term g arises from the toroidal coupling of the main harmonic ξ to the side-band amplitude ξ^r_{m+1}. For $\xi(a) = 0$ we have

$$g = -C\beta' r^{m+1} I(\xi), \tag{7}$$

where $C = (1 + m)m^4 R_0^2(1 + \gamma M_0^2/2)^2/2n^2 a^{2m+2}$ and $I(\xi) = -\int_0^a r^{1+m}\beta'\xi\,\mathrm{d}r$.

3. Results

3.1. Numerical

3.1.1. Equilibrium. The analytical equilibrium of (1) was accurately reconstructed numerically with FINESSE [24] for various M_0. With $\gamma = 5/3$, $\epsilon = 0.1$ and β between zero at the plasma edge and a maximum $\beta \approx 5 \times 10^{-3}$, a relatively flat, monotonically increasing, safety-factor profile was obtained, which was centred around $q \approx 2$. The coefficients c_1 and c_2 of (1) were adjusted to make the height of the plasma cross-section at $R = R_0$ equal its width $2a$.

3.1.2. Continuum modes. The MHD spectrum for $n = 1$ was investigated with PHOENIX [21], including the poloidal harmonics $m = 0, 1, 2, 3$ and 4. The low-frequency continuous spectrum is shown in figure 1 as a function of the dimensionless radial coordinate $s \equiv \sqrt{(\psi - \psi_{\mathrm{m}})/(\psi_{\mathrm{e}} - \psi_{\mathrm{m}})} \approx r/a$.

Due to rotation and other toroidal effects, the low-frequency continuous spectrum deviates significantly from the uncoupled cylindrical continuum. Due to an intricate coupling [6, 11]

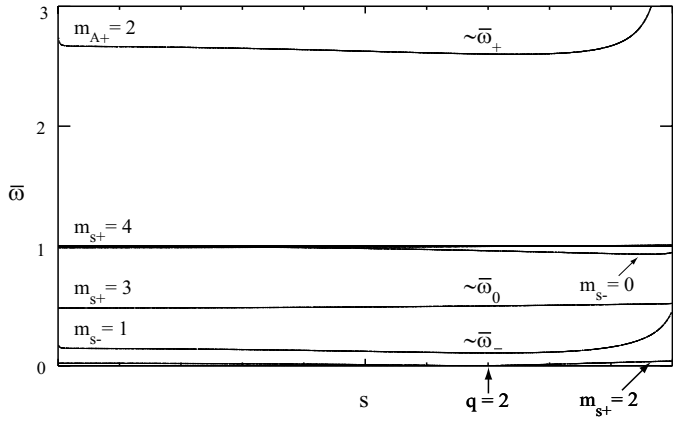

Figure 1. The low-frequency continuous spectrum for $M_0 = 1$. Here m is indicated for the Alfvén (A) and slow magnetosonic (s) waves, propagating in the co-rotating (+) or counter-rotating (−) direction. Global modes were found below $\bar{\omega}^2 = \bar{\omega}_\pm^2$.

with the $m_\mathrm{A} = 2$ and $m_\mathrm{s} = 3$ continuum branches, the $m_\mathrm{s} = 1$ continuum branch is dragged downwards in frequency near the rational surface and acquires an Alfvénic character. In a rotating equilibrium, the continuum does not reach $\bar{\omega} = 0$ but is lifted to a finite frequency. This frequency is analogous to the buoyancy frequency or Brunt–Väisälä-frequency [11] of an air parcel in a stably stratified atmosphere, with centrifugal forces replacing gravity.

The modified $m = 2$ Alfvén and $m = 1$ slow-wave continuum frequencies are described well by the frequencies $\bar{\omega}^2 = \bar{\omega}_\pm^2$ for which A_1 vanishes so that (3) becomes singular. The frequency range from $-\bar{\omega}_+$ to $\bar{\omega}_+$ is the BAE/GAM gap, modified by rotation. The gap between $-\bar{\omega}_-$ and $\bar{\omega}_-$ represents the TFI gap and is primarily due to the buoyancy effect mentioned above. Both gaps are clearly visible in figure 1. In the range $0.1 \leqslant M_0 \leqslant 1.6$, the frequencies $\bar{\omega}_-$ and $\bar{\omega}_+$ given by (5) were found to agree within a per cent with the gap frequencies obtained numerically.

3.1.3. Global Alfvén modes. Above certain Mach numbers, sequences of global modes were found to arise near the bottom and the top of the TFI gap, as shown in figure 2. Because of the low magnetic shear, these modes extend radially over the entire tokamak. They first appear near the bottom of the gap. At higher Mach numbers these modes also start to appear near the top of the gap.

Figure 3 shows the amplitudes of the first global mode. The Eulerian velocity perturbation $\boldsymbol{v} = -\mathrm{i}(\omega + n\Omega)\boldsymbol{\xi}$ is expressed in components as $2s\boldsymbol{v} = v_s\boldsymbol{a}_s - \mathrm{i}v_\vartheta\boldsymbol{a}_\vartheta - \mathrm{i}v_B\boldsymbol{a}_B$. Here $\boldsymbol{a}_s$ and $\boldsymbol{a}_\vartheta$ are covariant base vectors of the coordinate system (s, ϑ, ϕ) and $\boldsymbol{a}_B = qR\boldsymbol{B}/B_\phi = \boldsymbol{a}_\vartheta + qR\hat{\boldsymbol{e}}_\phi$ [21]. The v_ϑ-component is much larger than both v_s and v_B. Because this is the typical polarization for Alfvén waves, the observed modes can rightfully be called Alfvén modes. Figure 3 shows that the $m = 2$ component of v_s and v_ϑ, for which $(m/q - n)^2$ is minimal, is dominant. The v_B amplitude shows significant side-band amplitudes for $m = 1$ and $m = 3$ as well, because motion parallel to the magnetic field does not bend the field lines. Due to perfectly conducting wall boundary conditions at the plasma edge, the radial v_s velocity vanishes at $s = 1$.

Global modes also appear slightly below the BAE/GAM frequency. Above critical Mach numbers $M_0 \approx 0.9$ and $M_0 \approx 1.0$, these modes branch off the top and bottom of the continuum,

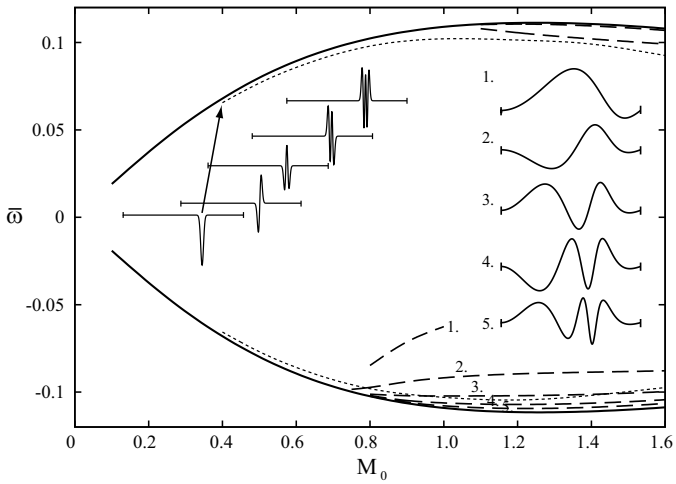

Figure 2. The frequencies of the TFI gap $\bar{\omega} \approx \pm\bar{\omega}_-$ (solid), the first zonal flow-like mode (dotted) and several global modes (dashed). The v_ϑ amplitudes of the first five zonal flow-like modes and the v_s amplitudes of the first five global modes are displayed for $M_0 = 1$. The first and second global modes were also found at the top of the gap.

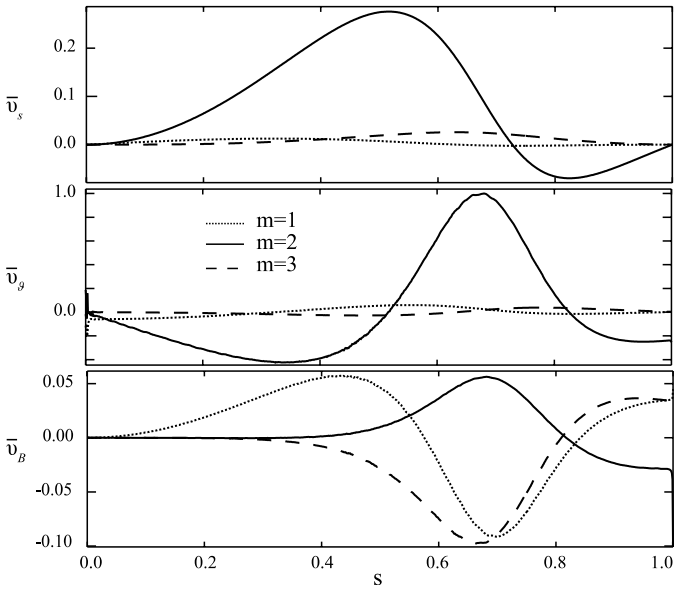

Figure 3. The velocity amplitudes $\bar{v}_i = \mathrm{Re}(v_i)/\mathrm{Re}(v_{\vartheta,\max.})$ of the first global mode near $\bar{\omega} = -\bar{\omega}_-$ for $M_0 = 0.8$.

respectively. The v_s and v_ϑ components are virtually indistinguishable from those of the global modes present in the TFI gap. The v_B-velocity, however, is significantly smaller because the frequency of these modes is well above that of sound waves ($\bar{\omega}_+ > 1$), which is too high for compressional wave motion in the direction of the magnetic field to be effective.

When the safety-factor profile is centred around $q = 1$ instead of 2, global $m = n = 1$ Alfvén modes appear near the bottom of the $\bar{\omega}_-$-gap already above $M_0 \approx 0.15$. To investigate

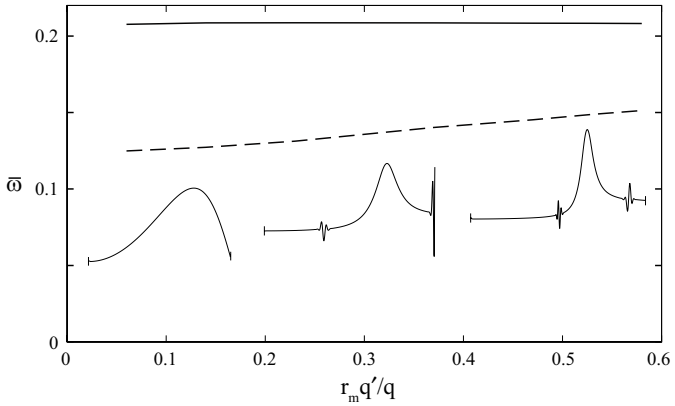

Figure 4. The frequencies of the $\bar{\omega}_-$ continuum (solid) and the first $m = n = 1$ global Alfvén mode (dashed) as a function of the magnetic shear $r_m q'/q$ for $M_0 = 1$, $q(r_m) = 1$ and $S = 10^8$. The v_ϑ-amplitude of the modes is shown for $r_m q'/q \approx 0.06$, 0.37 and 0.58, respectively.

how the magnetic shear influences these modes, we deviated from the analytical solution of (1) and chose $\frac{1}{2}d(RB_\phi)^2/d\psi = (1+\alpha)J(1-s^2)^\alpha$. By increasing α from 0 to 5, the magnetic shear was increased tenfold. From figure 4 one observes that, for the very low magnetic shear used in the foregoing simulations, the mode frequency seems to be more or less independent of the magnetic shear. For $r_m q'/q > 0.1$ the mode frequency increases approximately offset-linearly with the magnetic shear, towards the continuum frequency. Under the influence of magnetic shear, the modes also become more localized. Their frequency starts to overlap with the slow magnetosonic continuum so that under the influence of a finite resistivity η, the modes are damped [25]. For a Lundquist number $S \equiv B_0 R_0 \sqrt{\mu_0/\rho}/\eta = 10^8$, the rate at which the modes are damped is about two orders of magnitudes smaller than their frequency. The interaction with the slow continuum was predominantly found to affect the parallel v_B component and only a tiny perturbation of the v_s-component was observed. Note from figure 4 that the influence on the v_ϑ-component is largest near the plasma edge, where the Alfvén frequency diverges.

In order to test the robustness of these modes further, we increased the inverse aspect ratio and the dimensionless pressure to tokamak relevant values of $\epsilon = 0.3$ and a maximum $\beta \approx 0.04$. For these higher parameter values, the mode structure and frequency do not change substantially compared with the low-ϵ, low-β calculations. Also the modes discussed in the next section remain present.

3.1.4. Non-axisymmetric zonal flow modes. In figure 2 also localized but non-singular modes are shown to cluster near the continua, with an increasing number of nodes when moving in frequency towards the continuum (Sturmian in $\bar{\omega}^2$ [26]). These modes have a negligible radial velocity so that their motion is practically within the magnetic surfaces. Unlike the global Alfvén modes of the previous subsection, which exist only for Mach numbers above a threshold value, these localized modes seem to exist for all values of M_0. The frequency of these modes goes to zero with vanishing toroidal rotation, allowing us to identify them as a type of finite mode-number zonal flows. These modes arise due to compressibility of poloidal $\boldsymbol{E} \times \boldsymbol{B}$ perturbations which, if fully compensated by a parallel return flow, yields a zero-frequency perturbation. In agreement with the result of [27] for the axisymmetric case, these zonal flows acquire a finite oscillation frequency in the presence of toroidal rotation. This is primarily due to the previously mentioned centrifugal convective effect, which also gives the

$\bar{\omega}_-$-continuum its finite Brunt–Väisälä frequency. Simulations and analysis have shown [28] that a whole spectrum of finite-m, n zonal flows exist in general, that can condense into an axisymmetric $m = n = 0$ zonal flow. Similar to the modes found here, these flows were found to be radially located near rational surfaces.

3.2. Analytical

3.2.1. Mode existence criterion. Various features of the observed gap modes can be explained through (3). Multiplying (3) by ξ^* and integrating over the entire plasma yields

$$\int_0^a r^2 A_2' |\xi|^2 \, \mathrm{d}r = \int_0^a A_1 \left(r^3 \left|\xi'\right|^2 + r(m^2 - 1) |\xi|^2 \right) \mathrm{d}r + C \, |I(\xi)|^2 , \tag{8}$$

where the integrand $r^3 A_1 |\xi'|^2$ results from partial integration using $r^3 A_1 \xi' \xi^* |_0^a = 0$ and the last term is equal to $\int_0^a g \xi^* \, \mathrm{d}r$. To include magnetic shear, $(m/q - n)^2$ has to be added to A_1, so that for $A_1 > 0$ the right-hand side is manifestly positive. From (4) we see that A_1 is positive in the range $\bar{\omega}_0^2 < \bar{\omega}^2 < \bar{\omega}_+^2$ and for $\bar{\omega}^2 < \bar{\omega}_-^2$. For global modes to exist within this frequency range, therefore, a necessary condition is that

$$\int_0^a r^2 A_2' |\xi|^2 \, \mathrm{d}r = \frac{A_2}{\beta} \int_0^a r^2 \beta' |\xi|^2 \, \mathrm{d}r > 0. \tag{9}$$

For physical profiles the latter integral will be negative so this condition requires $A_2/\beta < 0$. Slightly below the continuum frequencies $\bar{\omega}^2 = \bar{\omega}_\pm^2$, where A_1 is positive but small, $A_2/\beta < 0$ can be written as

$$1 - q^2 \left(1 - \frac{\gamma}{2} M_0^2 - \frac{\gamma^2}{4} M_0^4 \right) > \frac{\gamma q^2}{n} \frac{2\bar{\omega} M_0}{1 - q^2 \bar{\omega}^2} \left(1 + \frac{M_0^2}{2} \right), \tag{10}$$

where $\bar{\omega} = \pm\bar{\omega}_-$ or $\pm\bar{\omega}_+$. The Mercier term $1 - q^2$ ensures that for $q = m/n > 1$, modes just below $\bar{\omega}^2 = \bar{\omega}_\pm^2$ only exist for sufficiently high M_0. This term represents the combined effect of the pressure gradient and the average toroidal magnetic field curvature, which for $q > 1$ gives a net stabilizing effect.

3.2.2. Comparison with simulations. Near $q = m/n = 1$, the destabilizing pressure gradient exactly cancels the stabilizing average field curvature so that (10) predicts that the rotation-induced Alfvén modes can already exist at relatively low Mach numbers. This was indeed found from simulations described in section 3.1.3. Modes were in this case absent near $\bar{\omega} = -\bar{\omega}_+$, for which (10) is not satisfied. For $\bar{\omega} = \bar{\omega}_+$, the right-hand side of (10) is negative and modes were found for Mach numbers as low as $M_0 = 0.1$.

The right-hand side of (10) is proportional to $\bar{\omega}\Omega$, which is typical for the Coriolis effect. For $\Omega > 0$, the Coriolis force favours the existence of modes at the bottom of the gap $\bar{\omega}^2 = \bar{\omega}_-^2$, in agreement with figure 2. For $\bar{\omega}^2 = \bar{\omega}_+^2$, modes at the top of the gap more easily satisfy the existence criterion of (10). Evaluating (10) for $q = m/n = 2/1$, we find that it is satisfied for $M_0 \geqslant 0.69$ when $\bar{\omega} = -\bar{\omega}_-$, $M_0 \geqslant 0.92$ for $\bar{\omega}_-$, $M_0 \geqslant 0.92$ for $-\bar{\omega}_+$ and $M_0 \geqslant 0.62$ for $\bar{\omega}_+$. These values are in agreement with the simulations and are very close to those for which modes appear in figure 2.

It is interesting to calculate the magnitude of the various terms of (8) from the simulations. For this purpose we use the $n = 1, m = 2$, v_s-component of the mode shown in figure 3. We find that numerically, the right-hand side approximately balances the left-hand side, with contributions more or less evenly distributed between the two integrals. The magnetic field-line bending contribution to the first integral of the right-hand side of (8) is an order of magnitude

smaller, in agreement with the observation that the mode shown in figure 3 does not show localization due to the magnetic shear.

Perhaps even more interesting is to show how the various components of A_2' from (4) contribute to the first integral of (8). The contribution of A_1' turns out to be negligible, in agreement with the assumption used in the analysis of section 3.2.1. The negative Mercier term $\beta'(m^2 - n^2)$ is only slightly smaller in magnitude than the positive flow drive $-\beta'(\gamma M_0^2/2 + \gamma^2 M_0^4/4)$. There is also quite a large positive contribution, about one third of the flow drive, from the Coriolis term of A_2'. This explains why in figure 2 modes were not found for $M_0 = 0.8$ near the bottom of the gap, where this term has negative sign.

3.2.3. Origin of the global Alfvén modes. The radial 'potential well' that enables the existence of global modes, is created by toroidal rotation through the term $r^2 A_2'$ in (3). Apart from a stabilizing Mercier term and the Coriolis contribution just discussed, A_2' contains a centrifugal term proportional to $-\beta'(\gamma M_0^2/2 + \gamma^2 M_0^4/4)$. This term is responsible for the existence of the global Alfvén modes, as is exemplified by the existence criterion (10). From the formulation of the Frieman–Rotenberg equation in [1], the effect of rigid toroidal rotation is, apart from a Doppler–Coriolis shift, the buoyancy-like centrifugal force $\boldsymbol{F} = \delta\rho R\Omega^2 \hat{e}_R$ due to an Eulerian density perturbation $\delta\rho = -\nabla \cdot (\rho\boldsymbol{\xi})$. To illustrate how a term like $-\beta'(\gamma M_0^2/2 + \gamma^2 M_0^4/4)$ can arise from this force, we consider the associated potential energy density $\delta W \equiv -\frac{1}{2}\boldsymbol{\xi}^* \cdot \boldsymbol{F}$ of an incompressible radial plasma displacement $\boldsymbol{\xi} = \xi^\psi \nabla\psi$

$$\delta W = \frac{1}{2} R\Omega^2 \frac{\partial\rho}{\partial\psi} |\xi^\psi|^2 (\nabla\psi \cdot \nabla R) \tag{11}$$

$$\approx p_0' \frac{\gamma M^2}{2} \left(1 + \frac{\gamma M^2}{2}\right) \frac{|\xi^\psi|^2}{R} (\nabla\psi \cdot \nabla R), \tag{12}$$

where the density $\rho = p_0(\psi) \exp(\gamma M^2/2)/T$ was expanded to $O(\gamma M^2/2)$. This expression for δW is reminiscent of the centrifugal term $-\beta'(\gamma M_0^2/2 + \gamma^2 M_0^4/4)$, responsible for the formation of the global modes. The singular continuum modes, in order to stay more or less incompressible, have only a very small radial component. The smoothly varying global modes can have a much larger radial perturbation so that they can make use of the energy source described by δW. When the volume average of δW is negative, a mode can gain energy from such a motion and depart from the continuum to form a discrete mode. Note that, because M increases outwards proportional to R, the plasma perturbation does not necessarily have to 'balloon' outwards to make use of this kinetic energy source.

3.2.4. Modes above the continua. The coefficient A_1 is negative in the frequency ranges $\bar{\omega}_-^2 < \bar{\omega}^2 < \bar{\omega}_0^2$ and for $\bar{\omega}^2 > \bar{\omega}_+^2$.

At frequencies away from the continua, when magnetic shear is low enough, A_1 may become negative enough for the first integral on the right-hand side of (8) to become negative. This is especially so when the mode frequency approaches $\bar{\omega}^2 = \bar{\omega}_0^2$ from below, for which A_1 diverges. In this case (8) gives, using $\int_0^a r^2 A_2' |\xi|^2 \, \mathrm{d}r = -A_2 I(r^{1-m}|\xi|^2)/\beta$,

$$A_2 > -C\beta \frac{|I(\xi)|^2}{I\left(r^{1-m}\,|\xi|^2\right)} \geqslant -C\beta I(r^{m-1}). \tag{13}$$

In the second step Schwarz's inequality is used to obtain a bound based only on 'known' quantities. In this case, toroidal rotation creates a potential *hill* for modes. The condition (13) can be relevant for RSAEs, which accumulate above $\bar{\omega}^2 = \bar{\omega}_+^2$ when the safety factor has a minimum near $q = m/n$. These modes are routinely observed in magnetic spectrograms as

up- or down-chirping Alfvén cascades [16, 17]. A characteristic bend in the spectral lines is observed near the minimum frequency $\bar{\omega}_+$ [9] which, depending on whether (10) is satisfied, may not be attainable.

4. Conclusions and discussion

In this paper we have shown analytically and numerically that, depending on the Mach number, global Alfvén eigenmodes can accumulate below or above the continuum frequencies $\bar{\omega}^2 = \bar{\omega}_-^2$ and $\bar{\omega}^2 = \bar{\omega}_+^2$. These new modes are distinctly different from TFAEs, which are formed by the coupling between an m-Alfvén wave and two $(m \pm 1)$-slow magnetosonic waves. Instead, the modes described in this work only have a single dominant poloidal mode number m and arise due to a 'potential well', created by toroidal rotation, close to the continua. Also the dependence of the mode frequency on the rotation frequency, linear for TFAEs, can be used to discriminate between them. The modes accumulating at $\bar{\omega}^2 = \bar{\omega}_+^2$ are in the same frequency range as BAEs. Because the mode equation, (3), is linear in β however, these modes cannot be said to be induced by a threshold value of β. Instead it is shown here that centrifugal forces are essential for their formation. An existence criterion (10), derived for negligible magnetic shear, shows that modes can exist below $\bar{\omega}^2 = \bar{\omega}_\pm^2$, near $q = 1$ at practically relevant toroidal rotation velocities. Simulations show that these modes remain present for practically relevant magnetic shear, aspect ratio, and β.

In addition to the stable modes described in this work, toroidal rotation was also found to induce unstable modes which will be reported in a forthcoming paper [29].

Very localized but non-singular modes observed in the simulations near $\bar{\omega}^2 = \bar{\omega}_-^2$ were identified as non-axisymmetric zonal flow modes. Because their motion is primarily within the magnetic surfaces, they do not contribute to radial transport and can play a role in storing some of the turbulent energy. Their negligible radial component is also the reason why they are not described by the mode existence criterion (10) for the radial component of the plasma perturbation. Because their amplitude is non-zero only in a small region around the magnetic surface these modes may escape strong continuum damping. When a small but finite resistivity was introduced the modes disappeared, however, from their original frequency range, while the global Alfvén modes were merely slightly damped.

In order to asses whether the global Alfvén modes described in this work can actually be experimentally observed, the implications of the various simplifying assumptions made in this work have to be investigated further. The effects of a finite temperature gradient and rotational shear, which were not taken into account in this work, enter the mode equation primarily through the Mach number. Ordinarily the Mach number decreases towards the plasma edge so that the term $r^2 A_2'$, responsible for the formation of modes, will only be larger than in the present case of constant M_0. A larger variation of the equilibrium quantities, or a smaller aspect ratio, will modify the continuum significantly, making continuum damping [25, 30] of the global modes inescapable. Ion Landau damping of the lower frequency modes is probably very small because their frequency $\bar{\omega}_- \ll 1$ is well below that of thermal ions. Similar to BAE modes [18], the modes near $\bar{\omega}^2 = \bar{\omega}_+^2$ may be destabilized by energetic (beam) ions. These modes may therefore arise in a hybrid regime, which is included as a third operating scenario for ITER. In this advanced tokamak operating regime, a broad low-shear region near $q = 1$ exists at the centre of a tokamak plasma.

When they are not destabilized, the newly discovered global modes may also prove to be useful. Because the frequencies $\bar{\omega}^2 = \bar{\omega}_\pm^2$ at which these modes accumulate depend sensitively on the Mach number, they can provide accurate information on the rotation velocity. Similar to how the sweeping of Alfvén cascades in reversed-shear plasmas provides information on

the q-profile, an extension of MHD spectroscopy can be envisioned in which the evolution of these modes provides information on the plasma rotation.

Acknowledgments

The authors thank J W S Blokland for his help with the numerical codes and J P Goedbloed for stimulating discussions. This work, supported by NWO, and the European Communities under the contract of the Association EURATOM/FOM, was carried out within the framework of the European Fusion Program. The views and opinions expressed herein do not necessarily reflect those of the European Commission.

References

[1] Waelbroeck F L 1996 *Phys. Plasmas* **3** 1047
[2] Wahlberg C and Bondeson A 2000 *Phys. Lett.* A **271** 285
[3] Rosenbluth M N and Rutherford P H 1975 *Phys. Rev. Lett.* **34** 1428
[4] Goedbloed J P *et al* 1993 *Plasma Phys. Control. Fusion* **35** B277
[5] Holst B v d *et al* 2000 *Phys. Rev. Lett.* **84** 2865
[6] Holst B v d *et al* 2000 *Phys. Plasmas* **7** 4208
[7] Chu M S *et al* 1992 *Phys. Fluids* B **4** 3713
[8] Turnbull A D *et al* 1993 *Phys. Fluids* B **5** 2546
[9] Breizman B N and Pekker M S 2005 *Phys. Plasmas* **12** 112506
[10] Winsor N, Johnson J L and Dawson J M 1968 *Phys. Fluids* **11** 2448
[11] Wahlberg C 2008 *Phys. Rev. Lett.* **101** 115003
[12] Heidbrink W W 2008 *Phys. Plasmas* **15** 055501
[13] Cheng C Z and Chance M S 1986 *Phys. Fluids* **29** 3695
[14] Appert K *et al* 1982 *Plasma Phys.* **24** 1147
[15] Berk H L *et al* 2001 *Phys. Rev. Lett.* **87** 185002
[16] Sharapov S E *et al* 2001 *Phys. Lett.* A **289** 127
[17] Edlund E M *et al* 2009 *Phys. Rev. Lett.* **102** 165003
[18] Heidbrink W W *et al* 1993 *Phys. Rev. Lett.* **71** 855
[19] Gorelenkov N N *et al* 2007 *Phys. Lett.* A **370** 70
[20] Maschke E K and Perrin H 1980 *Plasma Phys.* **22** 579
[21] Blokland J W S *et al* 2007 *J. Comput. Phys.* **226** 509
[22] Wahlberg C 2009 *Plasma Phys. Control. Fusion* **51** 085006
[23] Frieman E and Rotenberg M 1960 *Rev. Mod. Phys.* **32** 898
[24] Beliën A J C *et al* 2002 *J. Comput. Phys.* **182** 91
[25] Poedts S *et al* 1992 *Plasma Phys. Control. Fusion* **34** 1397
[26] Goedbloed J P 1975 *Phys. Fluids* **18** 1258
[27] Wang S 2006 *Phys. Rev. Lett.* **97** 129902
[28] Hallatschek K 2000 *Phys. Rev. Lett.* **84** 5145
[29] Haverkort J W and de Blank H J 2011 Stability of localized modes in rotating tokamak plasmas *Plasma Phys. Control. Fusion* **53** at press
[30] Zonca F and Chen L 1992 *Phys. Rev. Lett.* **68** 592